Volume 2
Number 9
September 2024
Pages 2393–2718

RSC Sustainability

rsc.li/rscsus

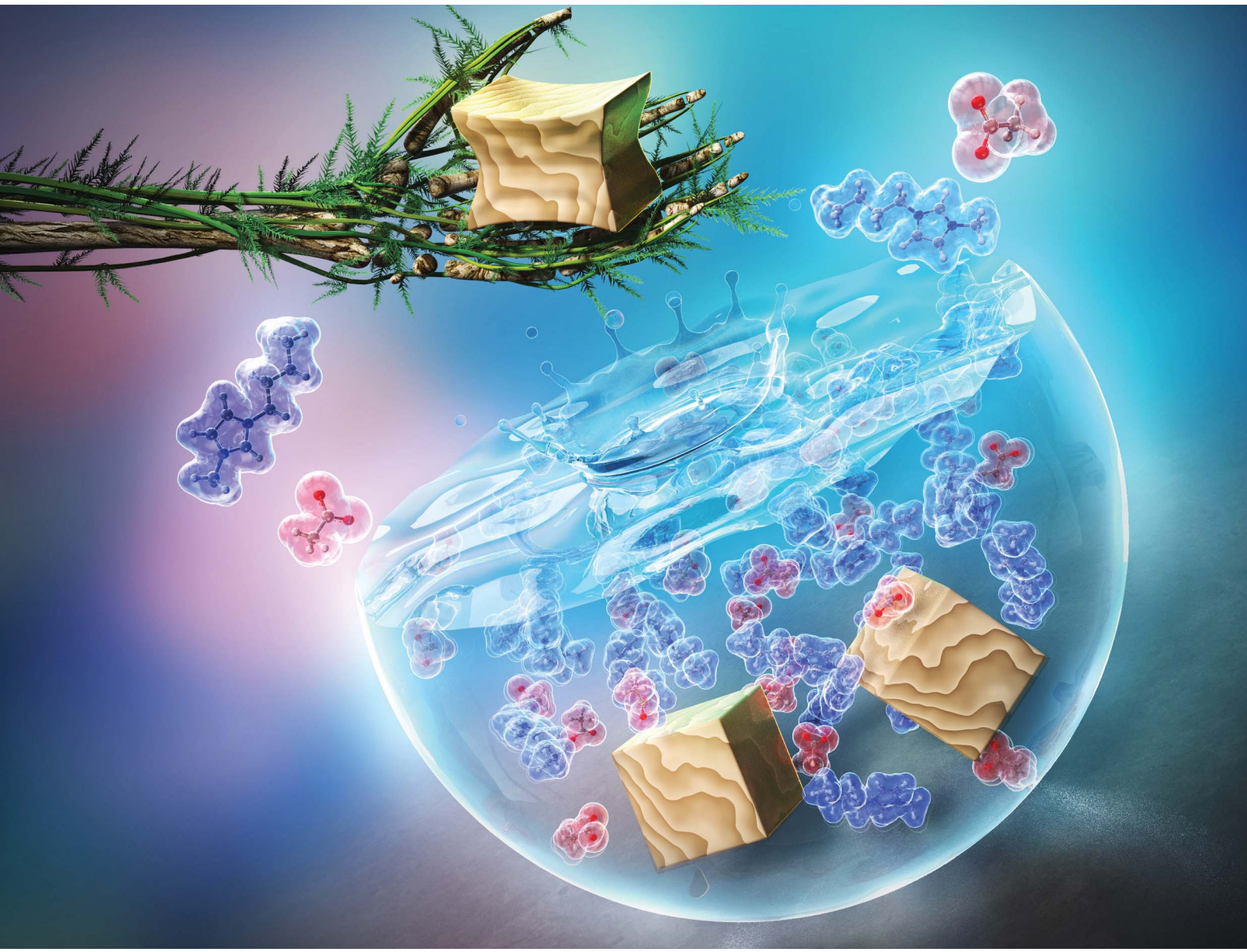

ISSN 2753-8125

ROYAL SOCIETY OF CHEMISTRY

COMMUNICATION

Hiroki Sakagami and Tetsuya Tsuda
Fabrication of biological cushioning materials with natural wood structure by an ionic liquid-based sustainable chemistry approach

RSC Sustainability

ROYAL SOCIETY OF CHEMISTRY

COMMUNICATION

View Article Online
View Journal | View Issue

Cite this: *RSC Sustainability*, 2024, **2**, 2486

Received 26th February 2024
Accepted 21st July 2024

DOI: 10.1039/d4su00097h

rsc.li/rscsus

Fabrication of biological cushioning materials with natural wood structure by an ionic liquid-based sustainable chemistry approach†

Hiroki Sakagami *[a] and Tetsuya Tsuda *[b]

While retaining wood morphology and characteristics, *i.e.*, growth rings and brown color, biological cushioning materials were successfully fabricated by the partial removal of lignin and hemicellulose from *Cryptomeria japonica* wood during an ionic liquid-based sustainable chemistry approach.

Sustainability spotlight

Cushioning materials are widely used for protecting fragile products in packaging and insulation. Most of these materials are petroleum-derived synthetic plastics. The consumption of such plastics often leads to problematic micro-sized plastic accumulation in the environment. For that reason, use of biological cushioning materials is strongly desired. One of the choices is to use the elastic softened wood (ESW). However, the preparation process for ESW usually requires severe conditions and laborious synthesis steps. Our approach for ESW preparation using ionic liquids enables processing with ease and less environmental impact. Moreover, it looks no different from the original wood. Our work contributes to the following UN sustainable development goals: responsible consumption and production (SDG 12).

Cushioning materials, *viz.*, elastic softened materials, are widely used for protecting fragile products in packaging and insulation. Most of these materials are petroleum-derived synthetic plastics, such as polyethylene, polypropylene polystyrene, polyamide, and polyurethane. However, the consumption of petroleum-based plastics leads to the accumulation of micro-sized plastics in the environment, which degrade slowly and have a long-term negative environmental impact.

Wood, which is recyclable and biodegrades quickly, is known to be an eco-friendly biomaterial used for building and furniture. Higher-density woods are generally preferred for manufacturing such wood products with high strength and hardness. But there are not many uses for lower-density woods, like balsa wood. Regardless of the type of wood, it is difficult to apply wood as a cushioning material, because of the irreversible damage to the rigid cell walls in which lignin is embedded with cellulose and hemicellulose polysaccharides. Many industrial cushioning materials, *e.g.*, sponge, composed of petroleum-based plastics, have uniformly dispersed small spaces (cells) that help shape recovery after compression. Wood naturally builds up with a similar cell structure with hierarchical pores with square and hexagonal cross-section-shaped fiber cells. The natural cellular distribution of wood is advantageous for the development of bio-based sponges. The use of wood as a sponge material requires softening the cell walls of the wood so that it can be compressed without damage at small loads.

The most common wood softening treatment is heat treatment under moist conditions. Under conditions where the wood has absorbed sufficient water, lignin and hemicellulose soften at 80–100 °C [1,2] and room temperature,[3] respectively.

By using these features, it becomes possible to manufacture furniture by bending[4] and compressing[5,6] the wood under hot and humid conditions without damaging it. However, wood materials softened at high temperatures spontaneously return to a rigid state at room temperature, making it difficult to apply them as alternative cushioning or sponge materials. Another well-known wood softening process, chemical delignification treatment, can give the softness to wood at room temperature. However, the chemicals used for the delignification treatment of wood are potentially dangerous,[7–13] and the treatment processes are complicated.[9–13] Additionally, the warm brown appearance of wood, which many people like, is drastically changed to white, originating from the color of cellulose.

Herein, we describe a simple sustainable chemistry approach with ionic liquids (ILs) for producing elastic softened wood (ESW) that is usable as a cushioning material (Fig. 1a). ILs are liquid salts at temperatures below 100 °C and exhibit unique

[a]*Department of Agro-environmental Sciences, Faculty of Agriculture, Kyushu University, 744 Motooka, Nishi-ku, Fukuoka 819-0395, Japan. E-mail: h-sakagami@agr.kyushu-u.ac.jp*

[b]*Department of Materials Science, Graduate School of Science and Engineering, Chiba University, 1-33 Yayoicho, Inage-ku, Chiba 263-8522, Japan. E-mail: ttsuda@chiba-u.jp*

† Electronic supplementary information (ESI) available: Experimental details, additional data (Fig. S1–S3 and Table S1), and video clip (Movie S1). See DOI: https://doi.org/10.1039/d4su00097h

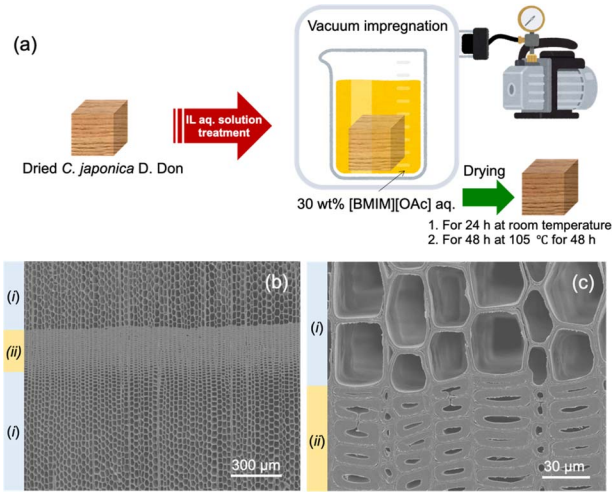

Fig. 1 (a) Schematic illustration of the IL aq. solution treatment process for fabricating ESWs and (b) SEM image of the cross-section view of the test piece prepared from *C. japonica* wood; (i) earlywood and (ii) latewood. (c) Enlarged SEM image of (b).

characteristics, including negligible vapor pressure, high flame resistance, relatively high ionic conductivity, and high chemical stability. ILs are also widely known as eco-friendly and sustainable chemicals that can be easily recycled owing to their negligible volatility. In the present study, we selected 1-butyl-3-methylimidazolium acetate ([BMIM][OAc]) as an IL for the IL-based approach, because [BMIM][OAc] can efficiently dissolve lignocellulose, including lignin and hemicellulose, under mild conditions[14,15] and be synthesized at a lower cost compared to other commonly used ILs with fluoroanions. The dissolution of cell walls was investigated *via* FT-IR analyses, and the morphological characteristics of cells before and after compression were observed using a scanning electron microscope (SEM). The compressive strength and shape recovery after compression of resulting ESW specimens were evaluated by compression tests.

As the target tree, *Cryptomeria japonica* (*C. japonica*), which has a higher density (*ca.* 400 kg m^{-3}) than balsa wood (*ca.* 140 kg m^{-3}) and a standard wood appearance, was employed. Fig. 1b and c show typical SEM images of *C. japonica* used for the test piece. Wood, including *C. japonica*, is composed of hollow tubular fiber cells (called tracheids in softwood) arranged in a radial direction after division from cambial cells. The wood structure of *C. japonica*, which is simple and consists of three tissues, tracheids, ray parenchymas and resin cells, is formed with a distinct growth ring boundary composed of a dense latewood region with thick cell walls of tracheids and a sparse earlywood region with thin cell walls of tracheids throughout the four seasons of growth in a year. The average oven-dried density of wood specimens used in this study was 0.37 g cm^{-3} (370 kg m^{-3}), yielding a calculated void volume of *ca.* 75%, considering that the specific gravity of the wood substances is *ca.* 1.5. In other words, the maximum compression ratio can be estimated at *ca.* 75%.

After applying the IL-based sustainable chemistry approach to *C. japonica*, the resulting wood specimens retained the wood characteristics, *i.e.*, growth rings and brown color. However, the color becomes slightly darker than the original test piece. Fig. 2a shows a series of photographs for deformation behavior of a typical specimen obtained by our approach during compression–decompression with fingers. Since it was easily deformed, we determined that ESW was obtained. Interestingly all specimens prepared in this research easily compressed and recovered to their original shape immediately after the release of the compressive force. In order to clarify why ESW was obtained, the investigation was carried out using spectroscopic techniques. FT-IR spectra of the [BMIM][OAc], ESW, air-dried control specimen, and washed ESW specimen in the wavenumber range of 900–1800 cm^{-1} are shown in Fig. 2b. No discernible change except the spectrum related to [BMIM][OAc] was observed between the FT-IR spectra of ESW and the air-dried control specimen. Interestingly, after washing ESW with water, the FT-IR spectrum at approximately 1655 and 1725 cm^{-1} relatively decreased compared to the control specimen. When delignified wood and softened wood are produced by removing lignin and hemicellulose chemically,[7,9–13] in the course of the process, the reduction of the FT-IR peaks at 1670 and 1660 cm^{-1}, which are generally attributed to the C=O stretching vibration of the carbonyl group of lignin, is reported.[16,17] The peaks at 1736 and 1730 cm^{-1} indicate the C=O stretching vibration of the acetyl group in hemicellulose.[11,17] The peaks at 1590, 1500, and 1460 cm^{-1} are assigned to the aromatic skeletal vibration of lignin, which did not change in this study, and also decrease upon delignification.[7,17] Results of our FT-IR measurements strongly suggest that [BMIM][OAc] partially dissolves lignin and hemicellulose. Therefore, the ESW obtained in this research would be formed by the partial removal of lignin and hemicellulose from original *C. japonica* during the IL-based sustainable chemistry approach.

In order to conduct a mechanical quantitative evaluation of the resultant ESWs, we used a universal testing machine, which displays the relationship between the compressive stress and

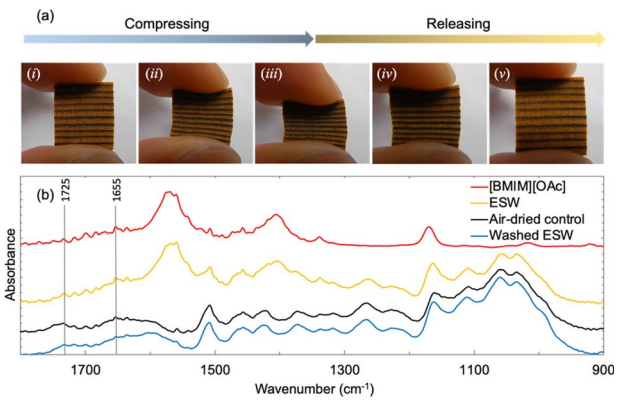

Fig. 2 (a) A series of photographs for deformation behavior (from (i) to (v)) of a typical ESW during compression with fingers. (b) FT-IR spectra of (red) IL ([BMIM][OAc]), (yellow) an ESW specimen, (black) an air-dried control specimen, and (blue) a washed ESW specimen.

compression ratio. Three water-absorbed specimens and three air-dried control specimens were also tested along with four ESW specimens, because the woods saturated with the liquids forming hydrogen bonds have a tendency to be softened with reversible chemical interaction with wood components. In most cases, the stress–strain curves of wood during compression in the radial direction are divided into an initial linear elastic region, a linear plateau region with a slow increase in stress, and a densification region with an accelerated increase in stress.[18,19] As shown in Fig. 3, common shape curves were recorded for the air-dried control and water-absorbed specimens. The curves of ESW specimens, however, displayed an extended linear plateau at low compressive stresses, rendering the elastic region indistinguishable. The average compressive stress at a 15% compression ratio for ESW (0.19 MPa) was *ca.* 5% of that recorded for the air-dried specimens (3.2 MPa) and *ca.* 10% of that for the water-saturated specimens (1.7 MPa). These compressive stress values of ESW in the radial direction are close to those reported for softened wood prepared by conventional chemical delignification treatments.[10]

The retention data of radial length after compression tests at a compression force of 1000 N and at 50% compression ratio are shown in Fig. S1 (ESI).† As to the compression tests at a compression force of 1000 N, the radial length of the air-dried control specimens after compression is *ca.* 55% of that before compression. Water-absorbed specimens show a higher retention of a radial length of *ca.* 80%. ESW has the highest retention value, *ca.* 90%, whereas those at 50% compression ratio showed *ca.* 100%. The compression ratio corresponds to the maximum value determined from the aforementioned calculation. In fact, the compression test condition under compression ratio over 70% caused permanent damage to ESW specimens. Evidence of this damage was observed at high ratios in the compressive stress–compression ratio curve (Fig. 3). Decreases in the compressive stress curve appeared for two ESW specimens at a compression ratio of approximately 66–68% due to slipping damage between the fiber cells. Thus, the retention of radial length of the ESW specimens at a compression ratio over 70% was reduced to approximately 88%, as shown in Fig. S1 (ESI).† Regarding the compression test at 50% compression ratio, as can be seen from Fig. S1 and Movie S1 (ESI),† retention was very close to 100%.

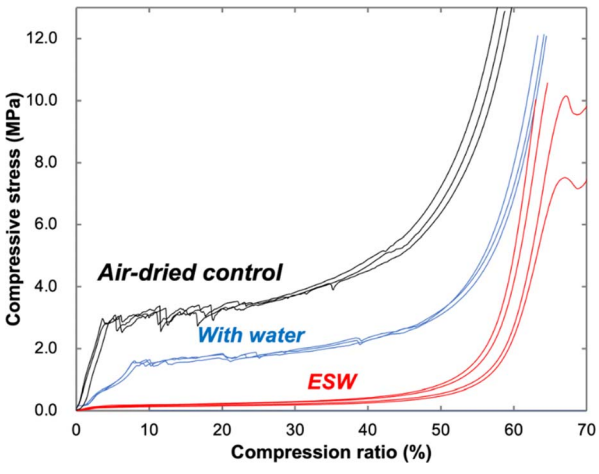

Fig. 3 Relationship between compressive stress and compression ratio during compression of (red) ESW, (blue) water-absorbed and (black) air-dried control specimens. These specimens were compressed at a speed of 2 mm min^{-1} under approximately 1000 N pressure.

SEM images of the prepared ESW are shown in Fig. S2 (ESI).† The substance embedding the cell lumens is the non-volatile [BMIM][OAc] that remains after the final drying process at 105 °C for 48 h (Fig. S2a (ESI)†). No significantly distorted distribution of cells or morphological changes were observed compared to the original *C. japonica* wood (Fig. 1b and c). However, microcracks were observed in the latewood region along with a growth ring boundary. Microcracking occurred due to dissociation of the latewood cells at the compound middle lamella owing to unexpected larger swelling of the cell walls in aqueous [BMIM][OAc] solution as shown in Fig. S3 (ESI).† Fig. S3a–S3c (ESI)† show SEM images of an air-dried control specimen, an air-dried control specimen immersed in aqueous [BMIM][OAc] solution, and the prepared ESW, respectively. And then, the measurements of radial length for twelve cells in latewood at the same position were also conducted. The lumens in the tracheids in Fig. S3b (ESI)† were almost closed, and the area of the tracheids was increased because of the swelling of the cell walls in aqueous [BMIM][OAc] solution. The tracheids of the ESW had excessively expanded cell walls, crushing the lumens and leaving no distinguishable gap due to further swelling of the cell walls (Fig. S3c (ESI)).† The swelling of several latewood tracheids was measured in four places at each specimen. The average calculated percentages of radial swelling ratios for the air-dried control specimen immersed in aqueous [BMIM][OAc] solution and ESW specimens, as compared to the air-dried control specimen, increased by 8.6% and 17.4%, respectively. All the tracheids of the ESW were significantly swollen.

C. japonica wood composed of lamellar structure for a dense latewood region with thick cell walls and a sparse earlywood region is easily deformed by compressive stress in the radial direction from the weakest point. SEM images of deformed tracheids in the ESW specimens at compression ratios of 20% and 50%, and unloading condition are shown in Fig. 4. The weakest point where deformation of the cells initiated was in the earlywood region between growth rings (Fig. 4b). When the compression ratio reached 50%, almost all the earlywood region was deformed (Fig. 4c). Deformation of cell shapes in latewood or damage, such as cracks and slipping, is not recognized during (Fig. 4c) and after (Fig. 4d) the compressive load, supporting the complete shape recovery with 100% retention of radial length after the removal of the compression force (Fig. S1 (ESI)†). SEM observation showed that thin cell walls in earlywood could be easily deformed without damage after softening with [BMIM][OAc].

Softened wood *via* delignification can be produced by dissolution of the cell walls.[9–13] Several ILs, including [BMIM][OAc] used in this research, have been reported to dissolve certain chemical components of wood. In early studies on the

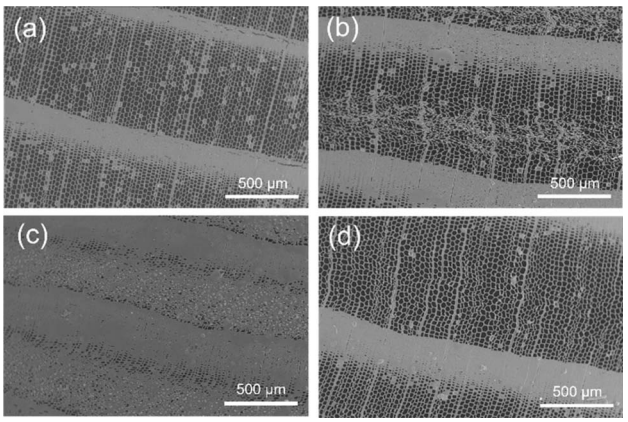

Fig. 4 SEM images of ESW: (a) before compression, under different compression ratios of (b) 20%, (c) 50% and (d) after unloading.

dissolution of lignocellulose with ILs, Swatloski *et al.*[20] and Pu *et al.*[21] demonstrated the dissolution of commercial or isolated cellulose and lignin, respectively. Subsequently, the dissolution of cellulose and lignin in finely divided wood shavings, such as pine, poplar, eucalyptus, and oak,[22] and the variable solubility of thermomechanical pulp from wood, ball-milled wood powder, sawdust, and wood chips,[23] were confirmed. Delignification enables the dissolution of large amounts of cell walls in latewood, whereas dissolution by ILs involves subsequent cell division after the extreme swelling of the cell walls.[24–29] These previous studies utilized optical microscopy to seek the changes in the appearance of cells in thin sections of wood. In our study, SEM observation of bulk wood specimens was conducted to shed light on the small cracks dividing cells and the swelling of the cell walls (Fig. S2 and S3 (ESI)†). But, formation of small pores[10] and thinning of the cell walls[9–13] *via* delignification were not verified on the micrometer scale although the dissolution of wood components was confirmed by FT-IR measurements (Fig. 2b).

Test pieces of *C. japonica* wood were softened using the sustainable chemistry approach with [BMIM][OAc]. The average radial compressive stress of ESW (0.19 MPa) was 5% of that for air-dried control specimens (3.2 MPa). ESW specimens retained almost 100% of their radial length after the removal of the compressive force, if the compression ratio is less than 50%. The FT-IR spectrum of a washed specimen of ESW showed a minimal decrease in the intensity of peaks at approximately 1655 and 1725 cm^{-1} compared to that of the control specimen, indicating the partial removal of lignin and hemicellulose. However, the dissolution of thin cell walls, a common consequence of delignification, was not confirmed after the IL-based approach. SEM observation revealed that the initially compressed cells were in the earlywood region. This suggests that the thin cell walls in earlywood can easily deform without irreversible damage, accompanied by minor mechanical softening caused by the partial dissolution of lignin and hemicellulose during the [BMIM][OAc] treatment. We concluded that *C. japonica* wood undergoes softening while retaining elasticity by the IL-based sustainable chemistry approach; thus, this ESW would be employed as an alternative to fossil-based plastic materials for cushioning and packaging applications.

Data availability

The data supporting the article titled, Fabrication of biological cushioning materials with natural wood structure by an ionic liquid-based sustainable chemistry approach, have been included as a part of the ESI.†

Author contributions

H. S. conducted the experiments and wrote the original draft. T. T. selected ILs and proposed the chemical treatment. Both authors contributed in review and editing of the manuscript.

Conflicts of interest

The authors have no conflicts to declare.

Acknowledgements

We thank the staff of the Kasuya Research Forest of Kyushu University for providing the wood materials. We also thank the staff of the Center of Advanced Instrumental Analysis, Kyushu University, for providing the infrared spectrometer used in this study. Part of this research was funded by a support program for young scientists at the Faculty of Agriculture at Kyushu University and projects, JPNP20004, subsidized by the New Energy and Industrial Technology Development Organization (NEDO) and JSPS KAKENHI Grant Number JP23K18547.

References

1 L. Salmén, *J. Mater. Sci.*, 1984, **19**, 3090.
2 T. Sadoh, *Wood Sci. Technol.*, 1981, **15**, 57.
3 W. J. Cousins, *Wood Sci. Technol.*, 1978, **12**, 161.
4 E. C. Peck, *Agric. Handb. 125*, Department of Agriculture, Forest Service, United States, 1957.
5 M. Inoue, M. Norimoto, M. Tanahashi and R. M. Rowell, *Wood Fiber Sci.*, 2007, **25**, 224.
6 R. Huang, N. Fujimoto, H. Sakagami and S. Feng, *J. Wood Sci.*, 2021, **67**, 43.
7 M. Frey, D. Widner, J. S. Segmehl, K. Casdorff, T. Keplinger and I. Burgert, *ACS Appl. Mater. Interfaces*, 2018, **10**, 5030.
8 R. Kumar, F. Hu, C. A. Hubbell, A. J. Ragauskas and C. E. Wyman, *Bioresour. Technol.*, 2013, **130**, 372.
9 J. Song, C. Chen, Z. Yang, Y. Kuang, T. Li, Y. Li, H. Huang, I. Kierzewski, B. Liu, S. He, T. Gao, S. U. Yuruker, A. Gong, B. Yang and L. Hu, *ACS Nano*, 2018, **12**, 140.
10 K. Wang, X. Liu, Y. Tan, W. Zhang, S. Zhang and J. Li, *Chem. Eng. J.*, 2019, **371**, 769.
11 C. Chen, J. Song, J. Cheng, Z. Pang, W. Gan, G. Chen, Y. Kuang, H. Huang, U. Ray, T. Li and L. Hu, *ACS Nano*, 2020, **14**, 16723.
12 Y. Wu, L. Yang, J. Zhou, F. Yang, Q. Huang and Y. Cai, *ACS Omega*, 2020, **5**, 22163.

13 Y. Cai, Y. Wu, F. Yang, J. Gan, Y. Wang and J. Zhang, *ACS Omega*, 2021, **6**, 12866.
14 H. T. Vo, C. S. Kim, B. S. Ahn, H. S. Kim and H. Lee, *J. Wood Chem. Technol.*, 2011, **31**, 89.
15 A. Casas, M. V. Alonso, M. Oliet, E. Rojo and F. Rodríguez, *J. Chem. Technol. Biotechnol.*, 2012, **87**, 472.
16 S. Kolboe and O. Ellefsen, *Tappi*, 1962, **45**, 163.
17 Y. Horikawa, S. Hirano, A. Mihashi, Y. Kobayashi, S. Zhai, J. Sugiyama and J. Appl, *J. Biochem. Biotechnol.*, 2019, **188**, 1066.
18 S. K. Maiti, L. J. Gibson and M. F. Ashby, *Acta Metall.*, 1984, **32**, 1963.
19 A. Reiterer and S. E. Stanzl-Tschegg, *Mech. Mater.*, 2001, **33**, 705.
20 R. P. Swatloski, S. K. Spear, J. D. Holbrey and R. D. Rogers, *J. Am. Chem. Soc.*, 2002, **124**, 4974.
21 Y. Pu, N. Jiang and A. J. Ragauskas, *J. Wood Chem. Technol.*, 2007, **27**, 23.
22 D. A. Fort, R. C. Remsing, R. P. Swatloski, P. Moyna, G. Moyna and R. D. Rogers, *Green Chem.*, 2007, **9**, 63.
23 I. Kilpeläinen, H. Xie, A. King, M. Granstrom, S. Heikkinen and D. S. Argyropoulos, *J. Agric. Food Chem.*, 2007, **55**, 9142.
24 H. Miyafuji and N. Suzuki, *J. Wood Sci.*, 2011, **57**, 459.
25 H. Miyafuji and N. Suzuki, *J. Wood Sci.*, 2012, **58**, 222.
26 T. Kanbayashi and H. Miyafuji, *J. Wood Sci.*, 2013, **59**, 410.
27 T. Kanbayashi and H. Miyafuji, *J. Wood Sci.*, 2014, **60**, 152.
28 J. Viell and W. Marquardt, *Holzforschung*, 2011, **65**, 519.
29 T. Tsuda, E. Mochizuki, S. Kishida, H. Sakagami, S. Tachibana, M. Ebisawa, N. Nemoto, Y. Nishimura and S. Kuwabata, *Electrochemistry*, 2012, **80**, 308.